

1-27-2010

Evaluating the Skeletal Chemistry of *Mytilus Californianus* as a Temperature Proxy: Effects of Microenvironment and Ontogeny

Heather L. Ford

University of California - Santa Cruz

Stephen A. Schellenberg

San Diego State University

Bonnie Becker

University of Washington Tacoma, bjbecker@uw.edu

Douglas L. Deutschman

San Diego State University

Kelsey A. Dyck

University of California - Santa Cruz

See next page for additional authors

Follow this and additional works at: https://digitalcommons.tacoma.uw.edu/ias_pub

 Part of the [Marine Biology Commons](#)

Recommended Citation

Ford, Heather L.; Schellenberg, Stephen A.; Becker, Bonnie; Deutschman, Douglas L.; Dyck, Kelsey A.; and Koch, Paul L., "Evaluating the Skeletal Chemistry of *Mytilus Californianus* as a Temperature Proxy: Effects of Microenvironment and Ontogeny" (2010). *SIAS Faculty Publications*. 10.

https://digitalcommons.tacoma.uw.edu/ias_pub/10

This Article is brought to you for free and open access by the School of Interdisciplinary Arts and Sciences at UW Tacoma Digital Commons. It has been accepted for inclusion in SIAS Faculty Publications by an authorized administrator of UW Tacoma Digital Commons.

Authors

Heather L. Ford, Stephen A. Schellenberg, Bonnie Becker, Douglas L. Deutschman, Kelsey A. Dyck, and Paul L. Koch



Evaluating the skeletal chemistry of *Mytilus californianus* as a temperature proxy: Effects of microenvironment and ontogeny

Heather L. Ford,^{1,2} Stephen A. Schellenberg,¹ Bonnie J. Becker,³
Douglas L. Deutschman,⁴ Kelsey A. Dyck,⁵ and Paul L. Koch⁵

Received 18 August 2008; revised 7 March 2009; accepted 20 August 2009; published 27 January 2010.

[1] Molluscan shell chemistry may provide an important archive of mean annual temperature (MAT) and mean annual range in temperature (MART), but such direct temperature interpretations may be confounded by biologic, metabolic, or kinetic factors. To explore this potential archive, we outplanted variously sized specimens of the common mussel *Mytilus californianus* at relatively low and high intertidal positions in San Diego, California, for 382 days with in situ recording of ambient temperature and periodic sampling of water chemistry. The prismatic calcite layer of eight variously sized specimens from each intertidal position were then serially microsampled and geochemically analyzed. Average intraspecimen $\delta^{18}\text{O}$ values significantly covaried only with temperature, whereas Mg/Ca values showed a strong and significant positive correlation with growth rate. To assess intra-annual variations in shell chemistry as proxy for MART, each specimen's $\delta^{18}\text{O}$ record was ordinated in the time domain and compared to the predicted isotopic equilibrium $\delta^{18}\text{O}$ values from environmental data. Observed specimen values were significantly correlated with predicted equilibrium values, but show ^{18}O enrichments of 0.2 to 0.5‰. In contrast, Mg/Ca values were poorly correlated with temperature due to significant positive relationships with growth rate and intertidal position. Within the extrapallial fluid, pH, carbonate solution chemistry, Rayleigh fractionation and/or an undetermined source of disequilibrium may cause $\delta^{18}\text{O}$ values to deviate from predicted equilibrium precipitation for ambient seawater. Despite this consistent ^{18}O enrichment, intraskeletal variations in $\delta^{18}\text{O}$ values readily characterize the instrumental MAT and 5–95% MART values, making *M. californianus* a valuable source of information for paleoceanographic reconstructions.

Citation: Ford, H. L., S. A. Schellenberg, B. J. Becker, D. L. Deutschman, K. A. Dyck, and P. L. Koch (2010), Evaluating the skeletal chemistry of *Mytilus californianus* as a temperature proxy: Effects of microenvironment and ontogeny, *Paleoceanography*, 25, PA1203, doi:10.1029/2008PA001677.

1. Introduction

[2] Many studies have sought to couple variations in oxygen isotope values ($\delta^{18}\text{O}$) and minor element ratios (Mg/Ca, Sr/Ca) to construct comprehensive environmental records of local water chemistry (e.g., seawater $\delta^{18}\text{O}$ and its covariance with salinity), local temperature, and global ice volume [Lea *et al.*, 2000; Lear *et al.*, 2000; Billups and Schrag, 2002; Dutton *et al.*, 2002]. Carbonate-secreting metazoans (e.g., molluscs and corals) have been of particular interest because their accretionary growth potentially records subseasonal to supradecadal environmental infor-

mation [Klein *et al.*, 1997; Cohen and Hart, 2004; Sosdian *et al.*, 2006]. While metazoan carbonate $\delta^{18}\text{O}$ values reflect both ambient temperature and seawater $\delta^{18}\text{O}$ values ($\delta^{18}\text{O}_{\text{seawater}}$), Mg/Ca values have been viewed as a more direct recorder of temperature. However, other microenvironmental (e.g., salinity, productivity) and biological factors (e.g., metabolic effects, growth kinetics) may affect the poorly understood controls upon and processes of Mg substitution within biogenic calcite. Some studies report direct relationships between minor element ratios and temperature (Mg/Ca [Klein *et al.*, 1996a]) or more complex relationships sensitive to specimen age (Mg/Ca [Freitas *et al.*, 2005]; Sr/Ca [Sosdian *et al.*, 2006; Surge and Walker, 2006]). In addition, environmental factors other than temperature (e.g., productivity, salinity) and biological factors (e.g., growth rate, metabolic efficiency) may influence minor element ratios in corals [Goodkin *et al.*, 2007], scallops [Lorrain *et al.*, 2005], venerids [Gillikin *et al.*, 2005], and mussels (*Mytilus edulis* [Rosenberg and Hughes, 1991; Vander Putten *et al.*, 2000]; *M. trossulus* [Klein *et al.*, 1996b]).

[3] In this study, we investigate intraskeletal $\delta^{18}\text{O}$ and Mg/Ca variations within the common intertidal mussel *M. californianus* to assess its potential as a recorder of mean

¹Department of Geological Sciences, San Diego State University, San Diego, California, USA.

²Now at Department of Ocean Sciences, University of California, Santa Cruz, California, USA.

³Department of Environmental Sciences, University of Washington, Tacoma, Washington, USA.

⁴Department of Biological Sciences, San Diego State University, San Diego, California, USA.

⁵Department of Earth Sciences, University of California, Santa Cruz, California, USA.

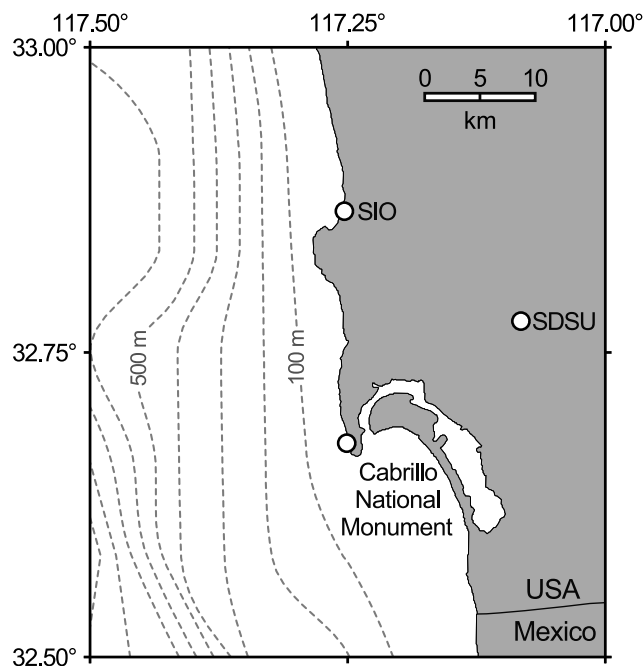


Figure 1. Study location within the intertidal zone of the Cabrillo National Monument of San Diego, California, USA. SDSU, San Diego State University; SIO, Scripps Institution of Oceanography.

annual temperature (MAT) and mean annual range in temperature (MART). Compared to previous studies using a limited number of subtidal-collected or aquarium-raised specimens [Klein *et al.*, 1996a; Wanamaker *et al.*, 2006; Freitas *et al.*, 2008], our experimental design comprised ontogenetic suites of specimens outplanted at relatively high and low intertidal positions, which better replicates the likely provenance of Holocene shell-midden specimens that are increasingly used in paleoceanographic and archeological investigations. This experimental design allowed direct assessment of the influence of intertidal position and growth rate on intraskeletal $\delta^{18}\text{O}$ and Mg/Ca variations within *M. californianus*.

[4] *Mytilus* is a common constituent of the Eastern Pacific intertidal zone and has been extensively studied because of its importance in aquaculture [Gosling, 1992a], usefulness as a monitor of water quality [Gordon *et al.*, 1980; Spangenberg and Cherr, 1996], and presence in archeological middens [Killingley, 1981; Walker *et al.*, 1999]. The valves of *Mytilus* consist of an outer organic periostracum layer, a middle prismatic calcite layer, and an inner nacreous aragonite layer [Taylor *et al.*, 1969]. Within the prismatic layer, faint growth bands corresponding to tidal periodicity are well documented in *M. edulis* [Richardson, 1989], and aid in growth transect microsampling for biogeochemical analyses. Previous studies investigating minor element ratios of the prismatic layer in intertidal *M. edulis* reported some Mg/Ca-temperature dependence that was interrupted by spring algal blooms [Vander Putten *et al.*, 2000], whereas a robust Mg/Ca-temperature calibration was reported for subtidal *M. trossulus* [Klein *et al.*, 1996a]. Here we choose to study *M. californianus* because its distribution

is largely restricted to the open coast [Robertson, 1964] compared to other *Mytilus* species that frequently inhabit bays and inlets where high frequency $\delta^{18}\text{O}_{\text{seawater}}$ variation is difficult to constrain [Klein *et al.*, 1996a]. *M. californianus* is also present in archeological middens, making it useful as a potential recorder of prehistoric changes in upwelling intensity, El Niño frequency, and coastal oceanography (e.g., MAT, MART). For example, *M. californianus* has been used to reconstruct modern upwelling events off San Diego [Killingley and Berger, 1979] and past oceanic circulation changes within the Santa Barbara Channel [Kennett *et al.*, 1997]. The wide distribution of the species (Aleutian Islands to northern Baja California, Mexico [Gosling, 1992b]) and its longevity (50–100 years in undisturbed patches [Suchanek, 1981]) make it a potentially rich archive of past environmental change.

2. Methods

2.1. Experimental Design

[5] To assess the influences of temperature, ontogeny, and intertidal position on the $\delta^{18}\text{O}$ and Mg/Ca values of *M. californianus* prismatic calcite, a natural population was collected from Scripps Institution of Oceanography Pier off La Jolla, California (N 32°52'0" W 117°15'5"; Figure 1) for preparation and outplanting into environmentally monitored intertidal positions within the ecological preserve of Cabrillo National Monument in San Diego, California (N 32°39'86," W 117°14'55"; Figure 1). Specimens were sorted into one of seven size bins based on their ventral margin length, which ranged from 24 to 73 mm (Figure 2). Outplant populations were produced by randomly drawing three specimens from each of the seven size bins. Each drawn specimen was photographed, mechanically labeled on the umbo, and lightly notched on the posterior margin with a Dremel hand drill. Outplant populations were deployed in cages at a lower intertidal position (LIP; -0.021 m Mean Lower Low Water (MLLW)) and an

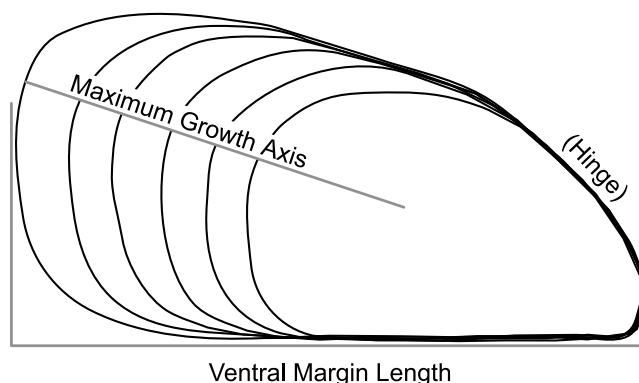


Figure 2. Line drawing of left valve of *Mytilus californianus* showing the ventral margin length (measured preoutplant and postoutplant to determine ventral extension; see Figure 4) and the maximum growth axis (along which outplant accretion length was measured; see Tables 1 and 2). Left valves were thin sectioned along their maximum growth axis to contiguously microsample the prismatic calcite precipitated during the outplant interval.

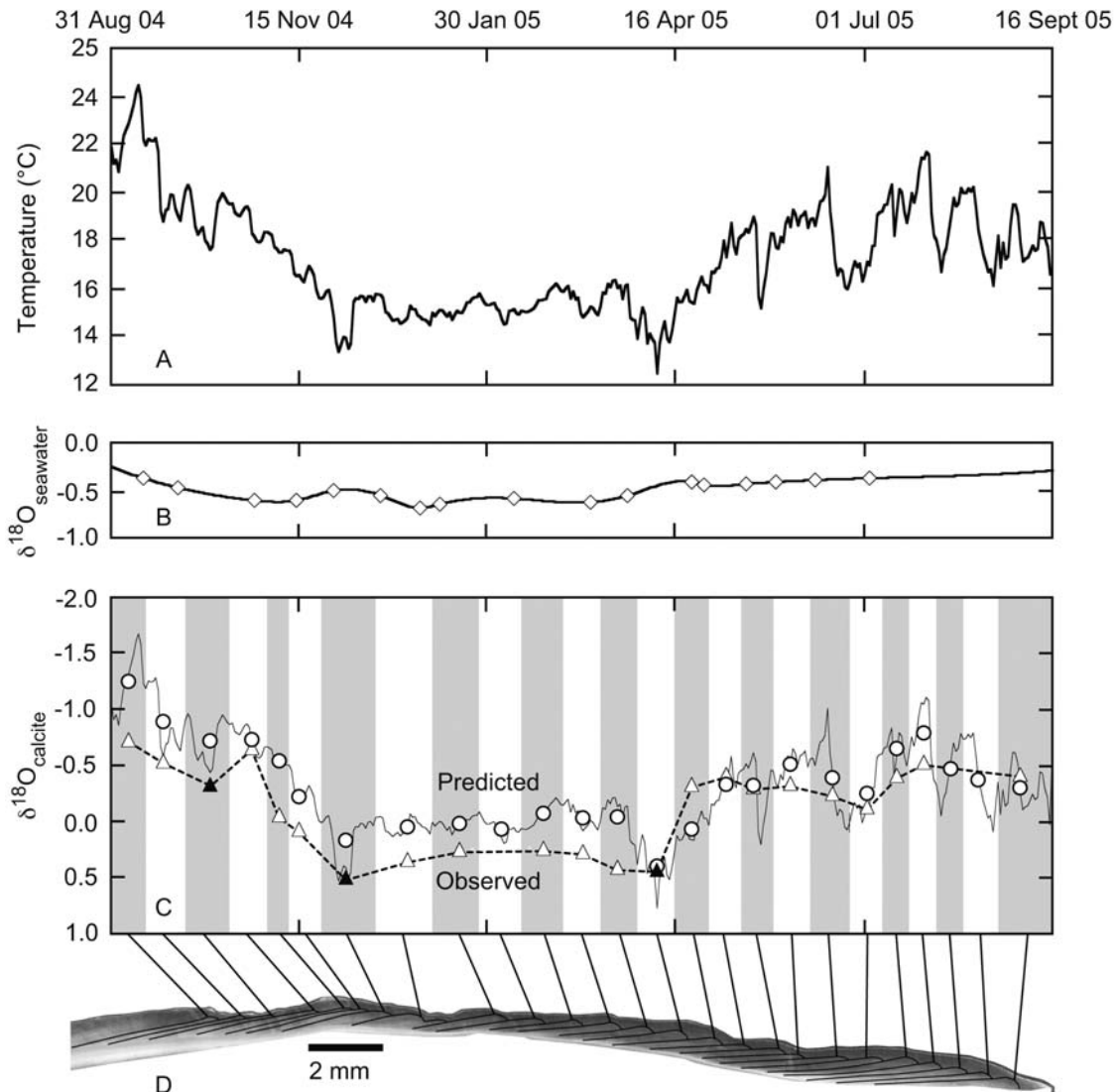


Figure 3. Construction of predicted $\delta^{18}\text{O}_{\text{equilibrium calcite}}$ record and comparison to observed $\delta^{18}\text{O}_{M. californianus}$ record for each specimen for the outplant interval. (a) Average daily submerged seawater temperature; (b) $\delta^{18}\text{O}_{\text{seawater}}$ values (VSMOW, open diamonds) and cubic spline curve (solid line); (c) predicted daily $\delta^{18}\text{O}_{\text{equilibrium calcite}}$ values (VPDB, solid line) and observed $\delta^{18}\text{O}_{M. californianus}$ variations for UIP specimen 3U.07 (VPDB, triangles with dashed line, where solid triangles indicate use of microsample as tie point (see text)). Alternating gray and white vertical bars define a series of temporal bins based on ordination in the time domain of contiguous microsamples from UIP specimen 3U.07, with average predicted $\delta^{18}\text{O}_{\text{equilibrium calcite}}$ values for each temporal bin shown as bin-centered open circles. (d) Mosaic of thin-section images for UIP specimen 3U.07 (outplant length, 33 mm; outplant accretion, 24.1 mm) prior to removal of the inner nacreous layer and subsequent microsampling of prismatic layer. Overlay lines on specimen define area of each microsample within the prismatic layer, and each microsample is tied to its corresponding temporal bin ($n = 25$ microsamples).

upper intertidal position (UIP; +1.097 m MLLW) within Cabrillo National Monument for an outplant interval of 31 August 2004 to 16 September 2005 (382 days).

2.2. Environmental Monitoring

[6] To construct a record of predicted equilibrium $\delta^{18}\text{O}$ calcite for the outplant interval, simplified temperature and interpolated $\delta^{18}\text{O}_{\text{seawater}}$ records were constructed from

environmental data. Temperature at the UIP was recorded every five minutes by an in situ data logger. This temperature record was culled to include only times of predicted UIP submergence based on reference to water level data from nearby Scripps Institute of Oceanography Pier (NOAA Tidal Station No. 9410230). The resulting submerged temperature record was then further simplified to a submerged average daily temperature record that varied between 12.5

and 24.5°C for the 382 day outplant interval with a grand average of $17.2 \pm 2.2^\circ\text{C}$ (Figure 3a, solid line).

[7] Seawater samples were collected within the intertidal zone of Cabrillo National Monument at $\sim 2\text{--}3$ week intervals for $\delta^{18}\text{O}_{\text{seawater}}$ analysis (Figure 3b, open diamonds). $\delta^{18}\text{O}_{\text{seawater}}$ values were determined by equilibration with CO_2 at 18.1°C using a Fredrickson-type water equilibrator interfaced with a Finnigan MAT 251 mass spectrometer at the University of California, Davis. $\delta^{18}\text{O}_{\text{seawater}}$ values were standardized relative to VSMOW and varied from -0.28 to -0.67‰ with an average of $-0.48 \pm 0.11\text{‰}$ (instrument precision $\pm 0.05\text{‰}$; Data Set S1).¹ To produce an estimated average daily $\delta^{18}\text{O}_{\text{seawater}}$ record comparable to the average daily submerged temperature record, these low-resolution $\delta^{18}\text{O}_{\text{seawater}}$ data were fit with a cubic spline function using MATLAB to extract 382 evenly spaced interpolated $\delta^{18}\text{O}_{\text{seawater}}$ values (Figure 3b, solid line).

2.3. Specimen Preparation and Microsampling

[8] Fifteen and seventeen specimens were recovered alive from the LIP and UIP, respectively. These specimens were identified, cleaned of their organic tissue, and rinsed with deionized (DI) water. Preoutplant and postoutplant ventral margin lengths were compared to determine ventral margin extension during the outplant interval (Figure 2).

[9] Analysis of Variance (ANOVA) was used to assess whether the preoutplant ventral margin length or the outplanted tidal position affected specimen growth within the outplant populations. During the outplant interval, ventral margin extension was highly dependent on both preoutplant ventral margin length (i.e., smaller younger specimens showed greater ventral margin extension; $F_{1,29} = 47.496$; $p < 0.001$) and intertidal position (i.e., LIP specimens exhibited greater ventral margin extension than UIP; $F_{1,29} = 16.245$; $p < 0.001$) (Figure 4). Slopes of ventral margin extension for the LIP and UIP are parallel, indicating that growth for LIP and UIP likely differed due to percent submersion and thereby the potential for feeding and growth.

[10] For shell chemistry analyses, eight shells from each intertidal position were chosen to span the observed range of preoutplant ventral margin lengths and ventral margin extension during the outplant interval. The preoutplant shell margin (as identified by notching and photographs) was scored across the maximum growth axis of the left valve to allow its identification in the thin section. Left valves were then embedded in epoxy, sectioned along their maximum growth axis (Figure 2) using a Buehler IsoMet 5000 Linear Precision Saw, and progressively hand polished with increasingly fine 3M WetorDry Sandpaper (320, 600, 800, 1000 grit). Section surfaces were mounted to glass slides, thin sectioned to $\sim 500\ \mu\text{m}$, hand polished down to a thickness of $\sim 400\ \mu\text{m}$ with WetorDry Sandpaper, rinsed with DI water, and air dried. The length of outplant accretion along the maximum growth axis was defined and measured from the thin section as the linear distance from the preoutplant shell margin and the physical shell

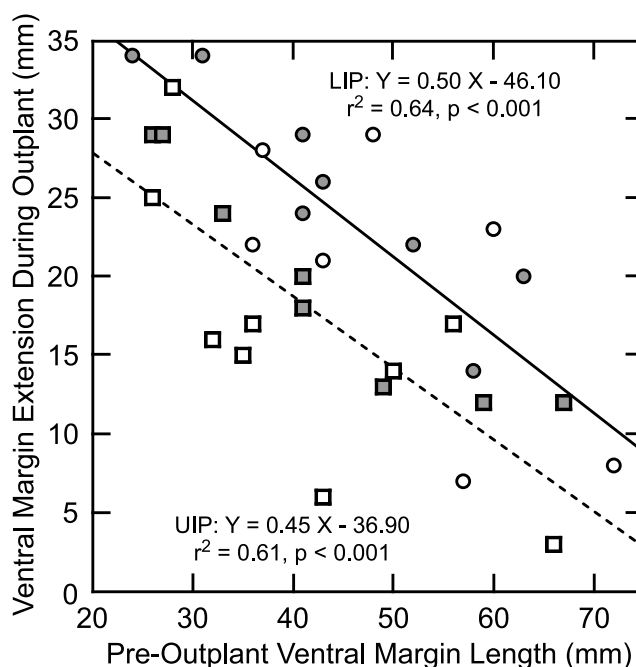


Figure 4. Reduced major axis regression between ventral margin extension during the outplant interval and the preoutplant ventral margin length for surviving individuals from the upper intertidal position (UIP, squares) and lower intertidal position (LIP, circles). Specimens used for subsequent intraskeletal analysis are indicated with gray fill.

margin. The epoxy and nacreous aragonite beneath the low-Mg prismatic calcite shell layer were removed from the thin section using a New Wave Research MicroMill. Shell material accreted within the prismatic calcite layer during the outplant interval was then contiguously microsampled following growth lines ($n = 22\text{--}45$ per shell, with more microsamples possible in the initially smaller, faster growing specimens); Figure 3d depicts microsampling paths for a large UIP specimen (3U.07). Each microsample was homogenized and split for Mg/Ca ($\sim 200\ \mu\text{g}$) and $\delta^{18}\text{O}$ ($\sim 50\ \mu\text{g}$) analysis; sampling resolution was primarily limited by these material needs.

2.4. Mg/Ca Analyses

[11] Microsample powder collected for minor element ratio analysis was placed in acid-cleaned 2 mL polypropylene microcentrifuge tubes and analyzed on a Perkin Elmer 4300 Dual View Inductively Coupled Plasma-Optical Emission Spectrometer (ICP-OES) at San Diego State University. Each microsample was acidified with 1 mL of 0.5 N trace metal grade HNO_3 to produce a $\sim 1\text{--}3$ mmol Ca solution. During each analytical run, four calibration standards with known Mg/Ca and Sr/Ca ratios were measured to span the general range of predicted minor element ratios in the unknown samples. In addition, these four calibration standards were diluted to low, medium and high calcium concentrations (Data Set S2) to confirm the absence of concentration effects on ICP-OES intensity ratios. Analytical blanks, consisting of the above 0.5 N trace-metal-grade HNO_3 as measured in

¹Auxiliary material data sets are available at <ftp://ftp.agu.org/apend/pa/2008pa001677>. Other auxiliary material files are in the HTML.

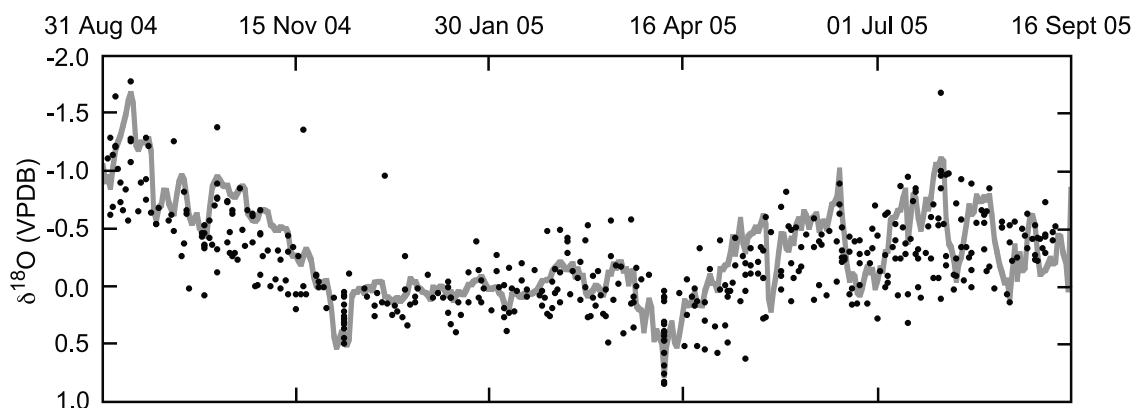


Figure 5. Observed $\delta^{18}\text{O}_{M. californianus}$ (black points) for all specimens plotted with predicted $\delta^{18}\text{O}_{\text{equilibrium calcite}}$ (gray curve; see Figure 3c). Most specimen values appear 0.2 to 0.5‰ enriched in ^{18}O compared to predicted equilibrium values.

random samples of the acid-cleaned 2 mL microcentrifuge tubes, were analyzed for matrix and background effects. A liquid consistency standard solution (LCS; i.e., ~ 2.0 mmol Ca solution; 62.3 mg of *M. californianus* prismatic calcite dissolved in 300 mL 0.5 N HNO_3) was routinely measured to monitor interrater and intrarun Mg/Ca reproducibility and produced a grand average of 4.86 ± 0.029 (0.59% RSD for 92 determinations over 9 analytical days; Data Set S3).

2.5. The $\delta^{18}\text{O}$ Analyses

[12] Microsample powder collected for stable isotopes was analyzed at the University of California, Santa Cruz, on a Micromass PRISM or OPTIMA mass spectrometer

interfaced common acid bath carbonate preparation system using 100% H_3PO_4 at 90°C . Calcite $\delta^{18}\text{O}$ values are reported relative to VPDB when plotted in Figures 3, 5, 6, 10, and 11 and subjected to statistical analysis and reported relative to SMOW for calculations involving water-calcite fractionation relationships (e.g., equation (2)). Conversions between VPDB and SMOW scales were calculated using the relationship (T. Coplen, personal communication, 2006) (see Text S1)

$$\delta^{18}\text{O}(\text{VPDB}) = (0.97001 * \delta^{18}\text{O}(\text{VSMOW})) - 29.29. \quad (1)$$

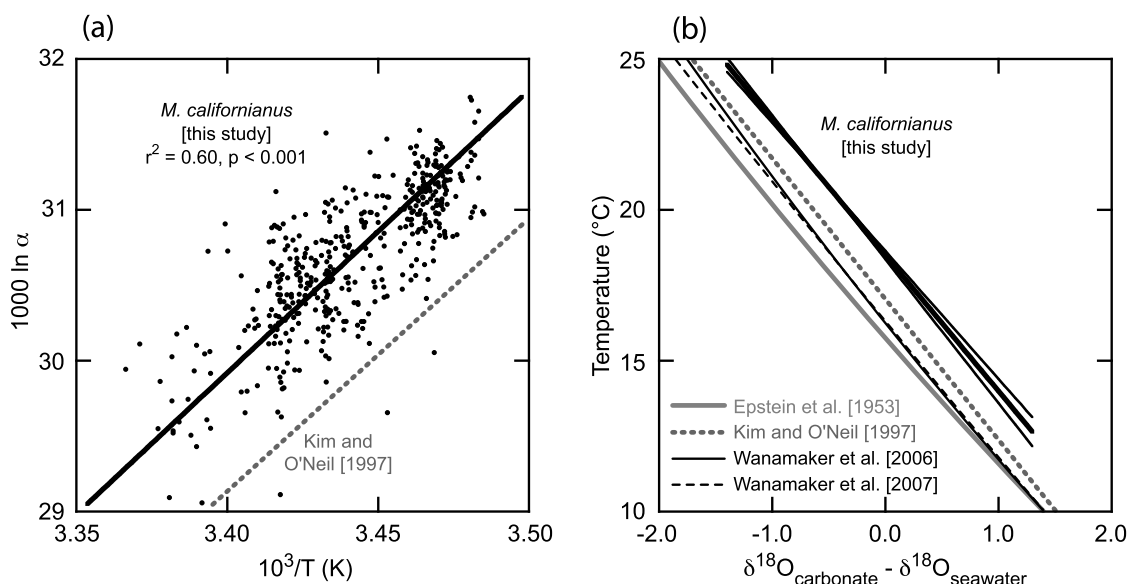


Figure 6. (a) Reduced major axis regression of temperature and α values for all $\delta^{18}\text{O}$ values of *Mytilus californianus* (black circles) and the temperature- α relationship for equilibrium $\delta^{18}\text{O}$ values of inorganic calcite (gray dashed line [Kim and O'Neil, 1997]). Equation (4) (see text) is α -based regression equation for *M. californianus*. (b) Reduced major axis regression of temperature and $\delta^{18}\text{O}$ values of *M. californianus* with 95% confidence envelope and $\delta^{18}\text{O}$ data omitted to facilitate comparison to $\delta^{18}\text{O}$ -temperature relationships from Epstein et al. [1953], Kim and O'Neil [1997], and Wanamaker et al. [2006, 2007]. Equation (5) (see text) is temperature-based regression equation for *M. californianus*.

Table 1. Summary Statistics for Intraspecimen Shell Chemistry^a

Tidal Position	Specimen ID	Outplant Accretion (mm)		Number of Mg/Ca Samples		Average Mg/Ca (mmol/mol)		5–95% Range Mg/Ca (mmol/mol)		Maximum Mg/Ca (mmol/mol)		Minimum Mg/Ca (mmol/mol)		Number of $\delta^{18}\text{O}$ Samples		Average $\delta^{18}\text{O}$ (‰)		5–95% Range $\delta^{18}\text{O}$ (‰)		Maximum $\delta^{18}\text{O}$ (‰)		Minimum $\delta^{18}\text{O}$ (‰)	
		Specimen	Accretion	Samples	Mg/Ca	Samples	Average	Samples	5–95% Range	Maximum	Minimum	Number	Average	5–95% Range	Maximum	Minimum							
Lower	3L01	34.2	29	4.58	29	1.67	5.56	3.49	26	-0.25	1.27	0.47	-0.96										
Lower	3L05	30.0	42	4.34	42	1.57	5.35	3.65	32	-0.20	1.19	0.45	-1.00										
Lower	3L09	31.3	45	4.99	44	2.42	6.80	3.75	35	-0.32	1.38	0.33	-1.78										
Lower	3L10	27.0	45	3.88	45	2.44	5.77	3.03	38	-0.20	1.52	0.85	-1.38										
Lower	3L13	25.6	28	4.67	28	1.65	5.64	3.65	21	-0.06	2.22	0.83	-1.68										
Lower	3L15	13.8	22	3.77	22	1.87	5.03	3.05	22	-0.13	1.15	0.39	-1.08										
Lower	3L16	23.3	45	4.32	45	2.16	5.70	3.24	40	-0.24	1.02	0.28	-1.26										
Lower	3L20	24.7	31	4.76	31	1.92	6.01	3.29	28	-0.09	1.12	0.76	-1.02										
Upper	3U02	28.3	37	5.18	37	1.85	6.33	4.25	34	-0.19	1.40	0.58	-1.22										
Upper	3U04	29.1	38	4.97	38	1.96	5.87	3.64	30	-0.37	1.23	0.26	-1.28										
Upper	3U07	24.1	25	4.51	25	1.12	5.23	3.84	22	-0.13	1.15	0.50	-0.73										
Upper	3U11	20.2	33	4.32	33	1.51	5.79	3.55	32	-0.41	1.29	0.14	-1.65										
Upper	3U13	21.6	29	4.01	29	1.08	4.71	3.30	11	0.04	1.33	0.69	-0.66										
Upper	3U14	14.9	27	3.99	27	2.44	6.12	2.98	26	-0.31	1.58	0.33	-1.29										
Upper	3U18	13.6	28	4.27	28	1.14	4.94	3.68	28	-0.15	0.97	0.47	-0.72										
Upper	3U20	14.5	25	4.40	25	1.99	5.77	3.57	24	-0.23	1.32	0.40	-1.14										

^aAll $\delta^{18}\text{O}$ values reported relative to VPDB.

[13] Analytical reproducibility ($\pm 1\sigma$; $n = 116$) was 0.06‰ for $\delta^{18}\text{O}$ and 0.04‰ for $\delta^{13}\text{C}$. $\delta^{13}\text{C}$ variations will be treated in a subsequent work.

3. Results

3.1. Bulk Intraspecimen Chemistry

[14] If *M. californianus* faithfully records ambient seawater temperature, then intertidal and ontogenetic factors should not affect its shell chemistry values. As a first test of this hypothesis, the average, 5–95% range, maximum, and minimum for $\delta^{18}\text{O}$ and Mg/Ca values for each specimen (i.e., intraspecimen values) were calculated (Table 1) and examined by ANOVA using experimental factors of accretion length (i.e., continuous variable along the maximum growth axis during the outplant interval; smaller specimens have higher accretion lengths) and intertidal position (i.e., categorical variable of UIP versus LIP) (Table 2).

[15] As summarized in Table 2, ANOVA results indicate that none of the $\delta^{18}\text{O}$ intraspecimen parameters were strongly or significantly influenced by the experimental factors, whereas some of the Mg/Ca intraspecimen parameters were affected. Accretion length shows a strong and significant positive relationship with average intraspecimen Mg/Ca. Accretion length and minimum intraspecimen Mg/Ca also showed a significant relationship, indicating that larger, slower-growing specimens have significantly lower minimum intraspecimen Mg/Ca values. Intertidal position also appeared to be a significant source of Mg/Ca variance, with UIP specimens having lower minimum intraspecimen Mg/Ca values. However, when the interaction of the experimental factors is considered by crossing intertidal position with accretion length, this relationship is nonsignificant (i.e., specimens that accrete less have lower Mg/Ca values independent of tidal position).

3.2. Matching Predicted and Observed $\delta^{18}\text{O}$ Records

[16] To test the fidelity with which each of the sixteen $\delta^{18}\text{O}$ time series from *M. californianus* recorded ambient temperature, a predicted daily equilibrium calcite $\delta^{18}\text{O}$ ($\delta^{18}\text{O}_{\text{equilibrium calcite}}$) record was constructed for the entire outplant interval by applying each pair of average daily submerged temperatures and estimated average daily $\delta^{18}\text{O}_{\text{seawater}}$ values to a temperature equation for inorganic calcite:

$$1000 \ln \alpha(\text{calcite-H}_2\text{O}) = 18.03(10^3 T^{-1}) - 32.42 + 0.25, \quad (2)$$

where T is in Kelvin, and

$$\alpha(\text{calcite-H}_2\text{O}) = \frac{(1000 + \delta^{18}\text{O}_{\text{equilibrium calcite}})}{(1000 + \delta^{18}\text{O}_{\text{seawater}})}, \quad (3)$$

where values are determined relative to VSMOW. Equation (2) is a modified version of the equation of Kim and O'Neil [1997] that accounts for a difference in the acid fractionation factor that they used relative to that used by most other workers (i.e., 0.25 was added to the intercept; see

Table 2. ANOVA Statistics for Intraspecimen Chemistry^a

	Outplant Accretion		Intertidal Position		Interaction	
	F _{1,13}	p Value	F _{1,13}	p Value	Outplant Accretion	Intertidal Position
δ ¹⁸ O Average	0.743	0.404	0.710	0.415		
δ ¹⁸ O Range	0.124	0.730	0.086	0.774		
δ ¹⁸ O Minimum	0.196	0.665	0.589	0.457		
δ ¹⁸ O Maximum	0.053	0.822	0.743	0.404		
Mg/Ca Average	11.70	0.005	2.899	0.112		
Mg/Ca Range	0.019	0.892	1.925	0.189		
Mg/Ca Minimum	7.269	0.018	6.334	0.026	F_{1,12} = 6.741; p = 0.023	F _{1,12} = 0.195; p = 0.667
Mg/Ca Maximum	2.041	0.177	0.018	0.896		

^aBold font denotes significance at the p = 0.05 level.

Text S1). These predicted δ¹⁸O_{equilibrium calcite} values are shown in Figure 3c as a solid line with open circles.

[17] The δ¹⁸O_{M. californianus} record of each specimen was then correlated to this predicted daily δ¹⁸O_{equilibrium calcite} record using various extrema in the δ¹⁸O_{M. californianus} records (e.g., Figure 3c, solid triangles). For each specimen, each of these “tie points” were assigned a corresponding outplant date, and all other δ¹⁸O_{M. californianus} values (and associated Mg/Ca values; see below) were linearly rescaled into this time domain by assuming constant growth between each pair of tie points.

[18] For each specimen, the time-averaged nature of each microsample required a comparable parsing and averaging of the higher-resolution predicted δ¹⁸O_{equilibrium calcite} record. To allow this comparison for each specimen, we assumed constant and continuous *Mytilus* growth between the above tie points, and converted the relative position of each microsample boundary to its corresponding relative outplant date. The resulting series of outplant dates defined contiguous temporal bins (i.e., Figure 3c, vertical bands) for which an average δ¹⁸O_{equilibrium calcite} value was calculated (Figure 3c, open circles). These δ¹⁸O_{equilibrium calcite} values were compared to their corresponding δ¹⁸O_{M. californianus} values in each bin using reduced major axis (RMA) regression (A. J. Bohonak and K. van der Linde, RMA: Software for reduced major axis regression—Java version, 2004, available at <http://www.kimvdlinde.com/professional/rma.html>) at three hierarchical levels: individual specimen, intertidal population, and entire population (Table 3). Individual specimen goodness of fit (r²) varied from 0.209 to 0.851, and all were significant. Intertidal population goodness of fit (r²) was 0.408 for LIP and 0.678 for UIP, and both were significant. Entire population goodness of fit (r²) was 0.514 and significant.

[19] The δ¹⁸O_{M. californianus} records for most specimens appear consistently enriched in ¹⁸O by +0.2 to 0.5‰ relative to the predicted δ¹⁸O_{equilibrium calcite} record (Figures 5 and S1). This ¹⁸O enrichment necessitated production of a species-specific *Mytilus californianus* temperature equation. To produce this equation, δ¹⁸O_{M. californianus} values (VSMOW) were paired with their average bin δ¹⁸O_{seawater} values (VSMOW) to calculate α values. RMA regression of the average bin temperature and bin α values for the entire population produced a

significant (r² = 0.60, p < 0.001; Figure 6a) correlation expressed by

$$1000 \ln \alpha (\text{calcite-H}_2\text{O}) = 18.734 \pm 0.564(10^3 \text{ T}^{-1}) - 33.776 \pm 1.941, \quad (4)$$

where T is in Kelvin and isotopic values are reported relative to SMOW.

3.3. Mg/Ca

[20] Mg/Ca values were compared to their corresponding average bin temperature by RMA regression at three hierarchical levels: individual specimen, intertidal population, and entire population (Table 3). Individual specimen goodness of fit (r²) varied from 0.001 to 0.438, and some specimens had significant regressions. Intertidal population goodness of fit (r²) was 0.044 for LIP and 0.087 for UIP, and both were significant. Entire population goodness of fit

Table 3. Reduced Major Axis Regressions Between δ¹⁸O_{M. californianus} and δ¹⁸O_{equilibrium calcite} and Between Mg/Ca and Temperature^a

	δ ¹⁸ O _{M. californianus} and δ ¹⁸ O _{equilibrium calcite}			Mg/Ca and Temperature		
	n	r ²	p Value	n	r ²	p Value
Entire Population	449	0.514	<0.001	528	0.058	<0.001
LIP Population	242	0.408	<0.001	286	0.044	0.001
UIP Population	207	0.678	<0.001	242	0.087	<0.001
3L.01	26	0.472	<0.001	29	0.173	0.025
3L.05	32	0.209	0.008	42	0.141	0.014
3L.09	35	0.758	<0.001	44	0.132	0.016
3L.10	38	0.476	<0.001	45	0.306	<0.001
3L.13	21	0.258	0.019	28	0.213	0.013
3L.15	22	0.681	<0.001	22	0.063	0.261
3L.16	40	0.367	<0.001	45	0.001	0.836
3L.20	28	0.534	<0.001	31	0.333	0.001
3U.02	34	0.851	<0.001	37	0.311	<0.001
3U.04	30	0.669	<0.001	38	0.301	<0.001
3U.07	22	0.712	<0.001	25	0.059	0.242
3U.11	32	0.687	<0.001	33	0.119	0.050
3U.13	11	0.739	0.001	29	0.089	0.116
3U.14	26	0.810	<0.001	27	0.388	0.001
3U.18	28	0.640	<0.001	28	0.004	0.751
3U.20	24	0.818	<0.001	25	0.438	<0.001

^aBoth δ¹⁸O_{M. californianus} and δ¹⁸O_{equilibrium calcite} are in ‰ relative to VPDB. Mg/Ca is in mmol/mol, and temperature is in °C. Bold font denotes significance at the p = 0.05 level.

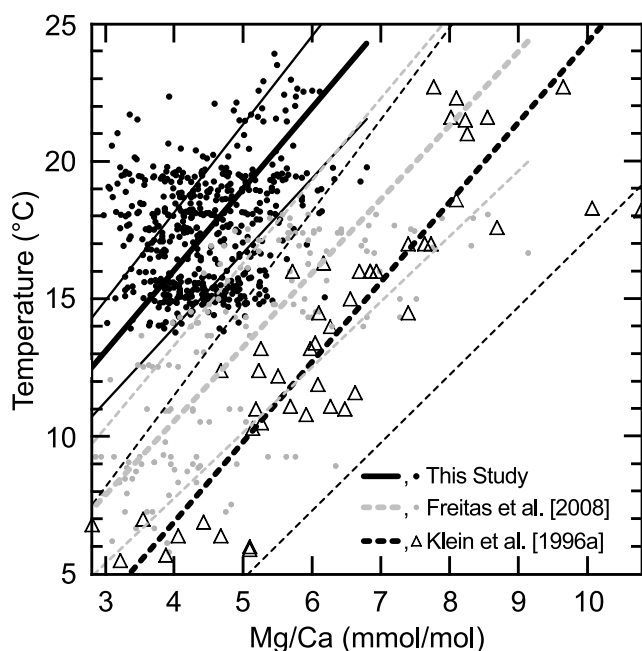


Figure 7. Mg/Ca-temperature relationships for *Mytilus californianus* from this study for 528 microsamples from sixteen variously sized specimens field cultured at two intertidal positions (data as solid black circles, reduced major axis regression as thick solid black line, and 95% confidence limits as thin solid black lines; $T = 4.209 (\pm 0.566) + 2.962 (\pm 0.125) \cdot \text{Mg/Ca} \text{ (mmol/mol)}$). Also plotted are Mg/Ca-temperature data from Freitas *et al.* [2008] for 154 microsamples from five similarly sized (2.0–2.7 cm initial length) *M. edulis* specimens field cultured by suspension one meter below water surface (data as solid gray circles, reduced major axis regression as thick dashed gray line, and 95% confidence limits as thin dashed gray lines; $T = 0.070 (\pm 0.293) + 0.373 (\pm 0.021) \cdot \text{Mg/Ca} \text{ (mmol/mol)}$) and from Klein *et al.* [1996a] for 46 microsamples from two *M. trossulus* specimens estimated to be three and four years old at start of outplant (no size reported) and field cultured under subtidal conditions (data as open gray triangles, reduced major axis regression as thick dashed black line, and 95% confidence limits as thin dashed black lines; $T = 1.616 (\pm 0.376) + 0.345 (\pm 0.030) \cdot \text{Mg/Ca} \text{ (mmol/mol)}$).

(r^2) was 0.058 and significant, with a RMA regression equation of

$$T(^{\circ}\text{C}) = 4.209(\pm 0.566) + 2.962(\pm 0.125) \cdot (\text{Mg/Ca}), \quad (5)$$

as expressed in Figures 7, 8, and S1.

4. Discussion

[21] Coupling metazoan carbonate $\delta^{18}\text{O}$ and Mg/Ca values is a potentially powerful means of reconstructing sub-seasonal to decadal variations in MAT, MART, and seawater $\delta^{18}\text{O}$ value, which may vary with the freshwater input to coastal systems. However, the modern systematics of these

potential proxies needs to be thoroughly understood to have confidence in their application to ancient records. Calibration studies have revealed that many metazoans precipitate skeletal carbonate at or very close to oxygen isotope equilibrium with seawater [Epstein *et al.*, 1953; Horibe and Oba, 1972; Grossman and Ku, 1986] or offset from equilibrium due to kinetic or other effects (e.g., 1 to 6‰ ^{18}O depleted in corals [McConnaughey, 1989a, 1989b]; ~ 1.3 ‰ ^{18}O enriched in barnacles [Killingley and Newman, 1982]). In contrast, calibration studies of Mg/Ca within and among metazoan clades show much greater variance, often requiring the development of taxon-specific calibrations of potentially limited environmental and geographic scope [Wefer and Berger, 1991; Lea, 2003]. Our study found a consistent offset from predicted isotopic equilibrium in $\delta^{18}\text{O}_{M. californianus}$, and identified confounding factors in the use of Mg/Ca paleothermometry related to biology (i.e., ontogenetic age as inferred by size) and environment (i.e., life position within the intertidal zone).

4.1. Bulk Shell Chemistry

[22] Bulk $\delta^{18}\text{O}_{M. californianus}$ data showed no interspecimen variation attributable to either accretion length or intertidal position. Lack of dependence on these experimental factors increases confidence in $\delta^{18}\text{O}_{M. californianus}$ as a temperature proxy. In contrast, statistical analysis of the Mg/Ca bulk chemistry of the specimens within our experiment revealed a strong ontogenetic factor that, if ignored, would bias paleoenvironmental reconstructions. Though mussel growth can be quite plastic [Seed and Suchanek, 1992], we assume specimen preoutplant length was a good approximation of ontogenetic age (i.e., larger specimens were older). Among our specimen population over the outplant interval, smaller specimens accreted significantly greater shell material, and this material was significantly higher in its average Mg/Ca. Gillikin *et al.* [2005] documented a similar pattern for the average annual Sr/Ca and annual growth rate in the veneroid butter clam *Saxidomus giganteus*, but not for the veneroid Northern quahog *Mercenaria mercenaria*. While determining a general mechanism to explain this positive relationship between growth rate and Mg/Ca in *M. californianus* is beyond the scope of this study, its presence confounds the direct interpretation of Mg/Ca as an absolute or relative temperature proxy without independent constraints on specimen growth rate. This sensitivity of Mg/Ca to ontogeny stands in stark contrast to the finding of some *Mytilus* studies [e.g., Klein *et al.*, 1996a] and is discussed further below.

4.2. Fidelity of *Mytilus* $\delta^{18}\text{O}$ and Temperature

[23] Several calibration studies have shown that many molluscs precipitate calcite in oxygen isotopic equilibrium with seawater [Epstein *et al.*, 1953; Horibe and Oba, 1972; Kirby *et al.*, 1998; Surge *et al.*, 2001]. However, conflicting studies within the family Pectinidae demonstrate precipitation in isotopic equilibrium (*Pecten maximus* [Chauvaud *et al.*, 2005]) or slightly offset from equilibrium ($\sim +0.7$ ‰; *Comptopallium radula* [Thébault *et al.*, 2007]) and dependent on growth rate ($\sim +0.4$ – 0.6 ‰; *P. maximus* [Owen *et al.*, 2002a, 2002b]). In this study, $\delta^{18}\text{O}_{M. californianus}$ values are consistently ^{18}O enriched by 0.2 to 0.5‰ relative to

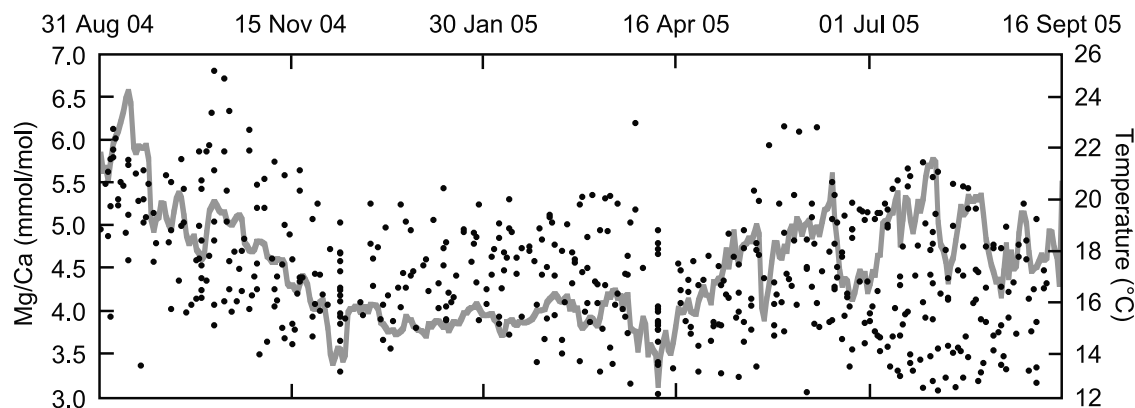


Figure 8. Mg/Ca (mmol/mol, black points) plotted with average daily submerged ambient seawater temperature (gray line) for outplant interval.

predicted $\delta^{18}\text{O}_{\text{equilibrium calcite}}$ values, a pattern undocumented in previous studies of intertidal *M. californianus* [Killingley and Berger, 1979; Killingley and Newman, 1982], subtidal *M. trossulus* [Klein et al., 1996a], or cultured *M. edulis* [Wanamaker et al., 2006; Freitas et al., 2008]. Killingley and Berger [1979] and Killingley and Newman [1982] estimated $\delta^{18}\text{O}_{\text{seawater}}$ values from local La Jolla salinity data using the salinity- $\delta^{18}\text{O}_{\text{seawater}}$ relationship for Pacific water from Craig and Gordon [1965]; however, this indirect method may have produced erroneously ^{18}O -enriched seawater $\delta^{18}\text{O}$ estimates if the coastal zone receives a significant freshwater flux. Differences between our study and the *M. trossulus* [Klein et al., 1996a] and *M. edulis* [Wanamaker et al., 2006; Freitas et al., 2008] studies could be attributed to the more naturalistic subaerial exposure of our *M. californianus* specimens or to metabolic and kinetic effects unique to *M. californianus*.

[24] Rayleigh fractionation during subaerial exposure and additional kinetic effects could account for the ^{18}O enrichment observed in *M. californianus*. Any water loss from the mantle by evaporation during subaerial exposure would preferentially remove the lighter ^{16}O , potentially generating ^{18}O enrichment of the extrapallial fluid (EPF; the fluid from which biogenic calcite precipitates) and producing ^{18}O -

enriched $\delta^{18}\text{O}_{M. californianus}$ values. As specimens experienced vastly different percent submersions (UIP: 24–46% versus LIP: 91–100% per half lunar cycle; Figure 9), a direct prediction of this scenario is that UIP specimens would be more ^{18}O enriched due to greater evaporative effects. However, no significant difference exists between the ^{18}O enrichment in populations from the two intertidal positions (Table 2). Other studies on multiple taxa have reported consistent ^{18}O enrichment independent of intertidal or subtidal position (e.g., barnacles [Killingley and Newman, 1982]; limpets [Schifano and Censi, 1983, 1986]). Therefore, other mechanisms may account for the ^{18}O enrichment as subaerial exposure seems an unlikely explanation for *M. californianus*.

[25] An alternate mechanism to account for this consistent ^{18}O enrichment involves metabolic control of EPF pH and the effect of pH on the distribution and stable isotopic composition of dissolved carbon species. At the calcification site, hemolymph (i.e., the body fluid that bathes tissues in open circulatory systems) supplies inorganic carbon to the EPF [Wheeler, 1992], which appears largely isolated from ambient seawater by a mantle-periostracum seal [Crenshaw, 1980]. Previous research on *M. edulis* and other bivalve species has demonstrated lower pH and higher

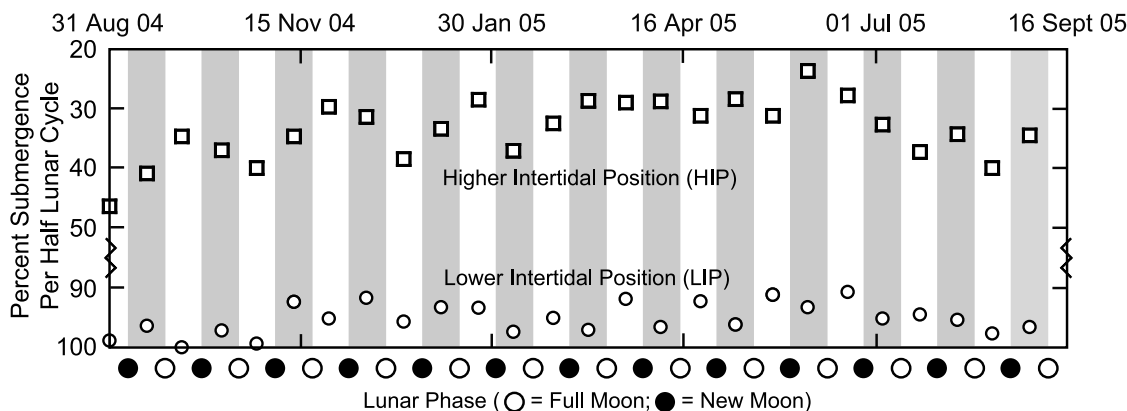


Figure 9. Percent submergence of upper intertidal populations (UIP, squares) and lower intertidal populations (LIP, circles) for each half lunar cycle during outplant interval of 31 August 2004 to 16 September 2005.

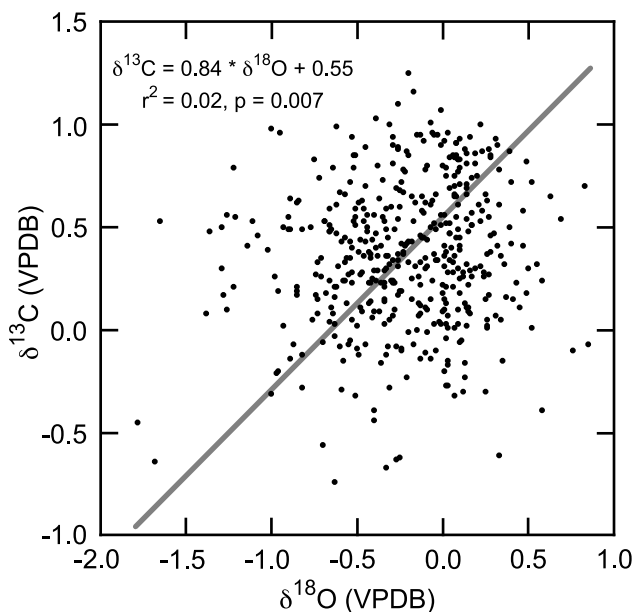


Figure 10. *Mytilus californianus* covariation in $\delta^{18}\text{O}$ and $\delta^{13}\text{C}$ values for all microsamples for sixteen specimens from UIP and LIP with reduced major axis regression and 95% confidence limits.

ΣCO_2 within the EPF relative to ambient seawater [Crenshaw, 1972]. pH has a significant role on the $\delta^{18}\text{O}$ value of calcite in foraminifera [Spero et al., 1997; Zeebe, 1999] and scallops [Owen et al., 2002b; Thébault et al., 2007], with increasing water-to-calcite oxygen isotope fractionation with decreasing pH. Thus metabolic control of the EPF composition may prove a viable mechanism for the observed ^{18}O enrichment. We note here that Kim and O'Neil [1997] consistently found that their calcite precipitated at higher supersaturations of Ca and HCO_3^- consistently showed slight ^{18}O enrichments relative to predicted equilibrium.

[26] In addition to such metabolic effects, biogenic calcite precipitation that deviates from predicted $\delta^{18}\text{O}_{\text{equilibrium calcite}}$ values are often attributed to kinetic effects [Urey, 1947; McConnaughey, 1989a]. Simultaneous depletion in heavy isotopes of C and O due to kinetic effects leads to quasi-linear relationships between skeletal $\delta^{18}\text{O}$ and $\delta^{13}\text{C}$ values during rapid calcification [McConnaughey, 1989a]. However, *M. californianus* specimens show a poor relationship between $\delta^{18}\text{O}$ and $\delta^{13}\text{C}$ values (study population: $r^2 = 0.016$, $p = 0.007$; best fit for a single specimen: 3U.20; $r^2 = 0.323$, $p = 0.004$; Figure 10) and $\delta^{18}\text{O}$ values are consistently enriched in ^{18}O , rather than depleted as expected for a kinetic effect.

[27] Despite the small offset relative to predicted equilibrium (Figure 6a) and other temperature calibrations (Figure 6b), $\delta^{18}\text{O}_{M. californianus}$ values and temperature are well correlated ($r^2 = 0.60$, $p < 0.001$; Figure 6a). *M. californianus* appears to have grown continuously through the outplant interval with no obvious growth shut down related to thermal stress or gametogenesis. Previous research has shown variations in growth rate attributed to seasonal variations in phytoplankton concentration (*M. edulis* [Page and Hubbard, 1987]) as well as temperature

and wave exposure (*M. californianus* [Blanchette et al., 2007]). With respect to gametogenesis, *M. californianus* spawns nearly continuously throughout the year, peaking from December to August [Suchanek, 1981; Petersen, 1984; Curiel-Ramírez and Cáceres-Martínez, 2004]. Given these physiological and ecological characteristics, *M. californianus* may prove a useful recorder of mean annual temperature (MAT) and mean annual range in temperature (MART).

[28] To assess the reliability of $\delta^{18}\text{O}_{M. californianus}$ values to record MAT and MART, the average, 5–95% range, minimum, and maximum values for $\delta^{18}\text{O}_{M. californianus}$ were applied to the species-specific $\delta^{18}\text{O}_{M. californianus}$ -temperature equation developed in this study (equation (4) and Table 4). Instrumental MAT was calculated as the average of the submerged average daily temperature record. *M. californianus* MAT ($17.4 \pm 0.5^\circ\text{C}$) confidently captures instrumental MAT ($17.2 \pm 2.2^\circ\text{C}$). This result is completely expected as equation (4) was derived using these data. Instrumental MART was calculated from the submerged average daily temperature record in two ways: the absolute minimum to maximum values (max–min) and the 5 and 95 percentile values (5–95%). Though the instrumental max–min MART (12°C) is underestimated, the instrumental 5–95% MART (7°C) is reasonably captured by the $\delta^{18}\text{O}_{M. californianus}$ max–min MART ($8.1 \pm 1.6^\circ\text{C}$) and the $\delta^{18}\text{O}_{M. californianus}$ 5–95% MART ($6.1 \pm 0.9^\circ\text{C}$). Underestimation of instrumental max–min MART is likely due to the time-averaged (~biweekly) nature of each microsample. Consequently, most specimens do not capture the full range of the high-resolution instrumental data, but do faithfully record instrumental MAT, and offer a reasonable proxy for some measure of MART.

4.3. Fidelity of *Mytilus* Mg/Ca and Temperature

[29] Development of a robust *M. californianus*-specific Mg/Ca-temperature equation is precluded by the poor correlation of Mg/Ca with ambient temperature ($n = 528$, $r^2 = 0.058$, $p < 0.001$; Figure 7). Unsurprisingly, Mg/Ca and $\delta^{18}\text{O}$ for the *M. californianus* population was also poorly correlated ($n = 448$, $r^2 = 0.186$, $p < 0.001$; Figure 11). We did not explicitly investigate potential seawater Mg/Ca variations over the outplant interval, but assume no significant variation based on previous studies [Klein et al., 1996a] and general principles of ocean chemistry [Drever, 1997]. In a study of comparable resolution, Klein et al. [1996a] developed an Mg/Ca-temperature calibration from two subtidal specimens of *M. trossulus* with a Mg/Ca range of 2.81 to 10.78 mmol/mol over a temperature range of 4 to 24°C compared to this study's *M. californianus* Mg/Ca range of 2.98 to 6.80 mmol/mol over a temperature range of 12.5 to 24.5°C . Application of Klein et al.'s [1996a] calibration to our Mg/Ca values produces a temperature range of 8 to 15°C , very different than the observed instrumental temperature range. Similarly, Freitas et al. [2008] developed an Mg/Ca-temperature calibration from laboratory (2.84 to 9.50 mmol/mol over a temperature range of ~ 12 to $\sim 18^\circ\text{C}$) and field cultured specimens (2.75 to 9.16 mmol/mol). These differences may arise from how different *Mytilus* species control the minor element composition within the EPF. For instance, Dodd [1965] found *Mytilus edulis diegensis* calcite had higher Mg concentra-

Table 4. Application of *M. californianus* Temperature Equation for MAT and MART^a

	Average α	MAT	Maximum α	Minimum α	Max–Min Temperature Range	Max–Min MART	95%	5%	5–95% Temperature Range	5–95% MART
Specimen 3L.01	1.03114	17.6	1.03185	1.03028	14.5–21.4	6.9	1.03177	1.03039	14.8–20.9	6.1
Specimen 3L.05	1.03124	17.1	1.03188	1.03025	14.4–21.5	7.2	1.03175	1.03035	14.9–21.1	6.2
Specimen 3L.09	1.03106	17.9	1.03169	1.02948	15.2–25.0	9.8	1.03166	1.03013	15.3–22.1	6.8
Specimen 3L.10	1.03115	17.5	1.03224	1.03005	12.9–22.4	9.6	1.03188	1.03049	14.3–20.4	6.1
Specimen 3L.13	1.03133	16.7	1.03225	1.02954	12.8–24.7	12.0	1.03203	1.03010	13.7–22.2	8.5
Specimen 3L.15	1.03125	17.1	1.03178	1.03019	14.8–21.8	7.0	1.03178	1.03057	14.8–20.1	5.3
Specimen 3L.16	1.03111	17.7	1.03165	1.02999	15.3–22.7	7.3	1.03159	1.03039	15.6–20.9	5.3
Specimen 3L.20	1.03128	17.0	1.03216	1.03018	13.2–21.8	8.7	1.03184	1.03067	14.5–19.6	5.1
Specimen 3U.02	1.03120	17.3	1.03197	1.02996	14.0–22.8	8.8	1.03180	1.03036	14.7–21.0	6.3
Specimen 3U.04	1.03102	18.1	1.03174	1.02995	15.0–22.9	7.9	1.03167	1.03029	15.3–21.4	6.1
Specimen 3U.07	1.03127	17.0	1.03194	1.03048	14.1–20.5	6.4	1.03192	1.03074	14.2–19.3	5.2
Specimen 3U.11	1.03099	18.2	1.03169	1.02952	15.2–24.8	9.7	1.03156	1.03019	15.7–21.8	6.1
Specimen 3U.13	1.03142	16.3	1.03208	1.03058	13.5–20.0	6.5	1.03198	1.03063	13.9–19.8	5.9
Specimen 3U.14	1.03107	17.9	1.03190	1.02997	14.3–22.8	8.5	1.03178	1.03002	14.8–22.5	7.8
Specimen 3U.18	1.03125	17.1	1.03186	1.03052	14.5–20.3	5.8	1.03178	1.03064	14.8–19.8	5.0
Specimen 3U.20	1.03118	17.4	1.03181	1.03004	14.7–22.5	7.8	1.03180	1.03039	14.7–20.9	6.2
Mussel Average		17.4 ± 0.5			14.3–22.5	8.1 ± 1.6			14.8–20.9	6.1 ± 0.9
Instrumental Temperature		17.2 ± 2.2			12.5–24.5	12.0			14.5–21.5	7.0

^aTemperature equation is $1000 \ln \alpha (\text{calcite-H}_2\text{O}) = 18.734 (10^3 \text{ T}^{-1}) - 33.776$. Specimen MAT is computed using the average $\delta^{18}\text{O}$ value for a single specimen (Table 1). Specimen maximum–minimum (max–min) temperature range is computed using the maximum and minimum observed $\delta^{18}\text{O}$ values. Specimen 5–95% temperature range is computed using the 5 and 95 percentiles of the observed $\delta^{18}\text{O}$ values. Instrumental MAT is the average of the submerged average daily temperature record. Instrumental MART is reported as max–min and 5–95% values for the submerged average daily temperature record.

tions relative to *M. californianus* in Southern California. (Note: *Mytilus edulis diegensis* is here assumed to be either native *M. trossulus* or invasive *M. galloprovincialis*, as taxonomic confusion and reevaluation of the *edulis* complex suggests *M. edulis* is not found on the North American Pacific coast [see Suchanek et al., 1997]). In addition, Dodd [1965] also found a strong size dependence for Mg concentration in *M. californianus*; prismatic calcite from the commissure edge of specimens 40–50 mm in length had higher Mg concentration than larger or smaller specimens. Owing to the differences in sampling techniques (sampling commissure edge versus bulk average chemistry), this pattern is not necessarily inconsistent with our result that smaller, faster-growing *M. californianus* have higher Mg/Ca values.

[30] Bivalves that precipitate low-magnesium calcite appear to strongly regulate Mg concentration within their extrapallial fluids given that the cation inhibits calcification [Berner, 1975]. Many calcification models have been proposed that emphasize the role of cation discrimination through ionic channels [Carré et al., 2006] and consider intercellular (between cell membranes, passive, low metabolic pumping) and intracellular (active, high metabolic pumping) pathways [Wheeler, 1992; Klein et al., 1996b]. In the model of Carré et al. [2006], Ca^{2+} transportation through the mollusc mantle via Ca^{2+} channels (passive transport proteins) may explain the relationship between mineralization rates and Sr^{2+} . With higher mineralization rates, the Ca^{2+} cation discrimination weakens and more Sr^{2+} leaks through the membranes. However, application of this model to Mg^{2+} transport is improbable because Mg^{2+} is poorly permeable through the Ca^{2+} channels [Lansman et al., 1986]. Conversely, the higher average Mg/Ca observed in faster growing *M. californianus* may be explained by the relative contribution of intercellular and intracellular transport of cations. Klein et al. [1996b] suggest intracellular

transport, which is more Ca^{2+} specific, is the dominant mode of transportation for slower growing, more metabolically efficient *M. trossulus* specimens. Higher Sr/Ca found in faster growing *M. trossulus* specimens was attributed to an increase in intercellular transportation. However, Gillikin et al. [2005] suggest the opposite would be true. An increase in metabolic pumping is related to an increase in Ca^{2+} -ATPase [Cohen and McConnaughey, 2003], which

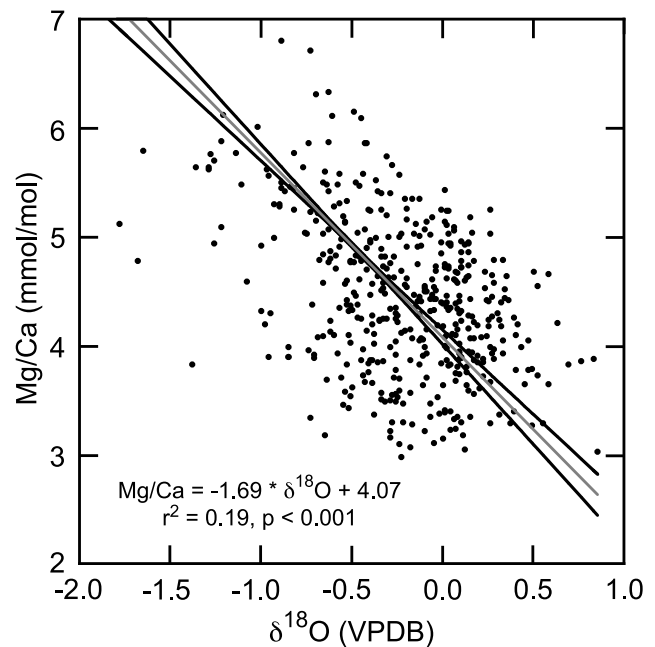


Figure 11. *Mytilus californianus* covariation in Mg/Ca and $\delta^{18}\text{O}$ values for all microsamples for sixteen specimens from UIP and LIP with reduced major axis regression and 95% confidence limits.

increases calcification rate and decreases Sr/Ca. As such, when calcification rate increases, Sr/Ca should decrease. Likewise, Carré *et al.* [2006] suggest that intercellular and intracellular transport are incapable of supplying the Ca^{2+} flux required for biomineralization. If Mg^{2+} transport functions similar to Sr^{2+} transport, alternative pathways or cation discrimination during crystallization must affect the Mg/Ca of *M. californianus*.

[31] Our results support a strong biological control on the Mg incorporation into the prismatic calcite layer of *M. californianus* that is independent of intertidal position, weakly dependent on temperature, and highly dependent on growth rate. Other bivalve studies have found minor element ratios to be inconsistent or poor proxies for ambient temperature. Freitas *et al.* [2005] found Mg/Ca ratios in the pecten *Pinna nobilis* to be a reliable temperature proxy for the initial 4–5 years of growth, but thereafter strong ontogenetic effects obscured any temperature signal. Freitas *et al.* [2006] found the Mg/Ca-temperature relationship of *Pecten maximus* to vary seasonally, with a negative relationship during autumn through early spring and a positive relationship during later spring through summer. In addition, strong metabolic controls on the incorporation of Sr/Ca have also been found for gastropods and bivalves in later ontogenetic stages (i.e., larger, slower-growing specimens [Klein *et al.*, 1996b; Purton *et al.*, 1999; Sosdian *et al.*, 2006]).

[32] Regardless of the exact physiological mechanisms, our modern intertidal calibration study demonstrated that Mg/Ca in *M. californianus* is strongly dependent on growth rate and is a poor direct proxy for temperature. Conversely, $\delta^{18}\text{O}_{M. californianus}$ values are strongly correlated with ambient temperature but slightly ^{18}O enriched relative to predicted $\delta^{18}\text{O}_{\text{equilibrium calcite}}$ values. With the exception of this study on outplanted intertidal specimens, studies of subtidal [Klein *et al.*, 1996a; Freitas *et al.*, 2008] and aquacultured [Wanamaker *et al.*, 2006] *Mytilus* have suggested that shell calcite formed in isotopic equilibrium of ambient seawater. Similarly, Klein *et al.* [1996a] found good correlation between Mg/Ca and temperature in two subtidal *M. trossulus* specimens. These differences among studies on the utility of $\delta^{18}\text{O}$ and Mg/Ca proxies may arise from differences in ecology (i.e., intertidal exposure), growth rates, or pH/carbonate solution chemistry within the EPF. Such complexities could be better understood with improved data on the general nature of calcification in a variety of environments (e.g., subtidal versus intertidal), growth rates, and the isotopic and elemental composition of EPF relative to ambient seawater.

[33] A primary goal of modern calibration studies is to determine the robustness of proxies for reconstructing paleoenvironmental conditions. The persistent presence of *M. californianus* in Native American shell middens may provide an archive of Holocene climate and upwelling history similar to the work on *Protothaca staminea* by

Takesue and Van Geen [2004]. Like the specimens in this study, their Native American midden material was likely drawn from the readily accessible intertidal zone. Given this fact, application of calibrations from modern subtidal or aquaculture experiments may produce biased reconstructions of paleoceanographic conditions if intertidal-exposure-related environmental and physiological factors affect isotopic fractionation and minor element partitioning within mussel shells.

5. Conclusions

[34] The ^{18}O variation within the calcite prismatic layer of the intertidal mussel *M. californianus* is a reliable monitor of temperature; however, an ^{18}O enrichment of 0.2 to 0.5‰ from $\delta^{18}\text{O}_{\text{equilibrium calcite}}$ values necessitated the development of a species-specific $\delta^{18}\text{O}$ -temperature equation. Using this equation, $\delta^{18}\text{O}_{M. californianus}$ values reasonably capture instrumental MAT as well as 5–95% MART by the minimum to maximum $\delta^{18}\text{O}_{M. californianus}$ values. In contrast, Mg/Ca in *M. californianus* is an unreliable temperature proxy based on a strong growth rate effect that produces higher values in smaller, faster-growing specimens. This growth rate effect undermines simple and direct coupling of *M. californianus* Mg/Ca and $\delta^{18}\text{O}$ values to deduce changes in water chemistry (salinity, $\delta^{18}\text{O}_{\text{seawater}}$), temperature, and global ice volume for paleoceanographic reconstructions.

[35] The deviation of $\delta^{18}\text{O}_{M. californianus}$ values from predicted equilibrium values highlights the need for further research to understand the controls on the EPF composition and the process of calcification. Unique pH and carbonate solution chemistry conditions different from ambient seawater, kinetic effects (related to growth rates), Rayleigh fractionation (possibly related to intertidal exposure), and/or an undetermined source of disequilibrium may have caused skeletal ^{18}O enrichment. Conflicting results as to the reliability of data from *Mytilus* species as temperature monitors highlight the need to further investigate environmental factors such as intertidal position (high, low, subtidal) and growth rates that may bias historical temperature reconstructions. *Mytilus* specimens recovered from Native American middens were likely harvested within the intertidal zone, and if researchers wish to use these natural archives to reconstruct accurate and precise seasonal to decadal records, microenvironmental- and growth-related proxy biases must be thoroughly examined.

[36] **Acknowledgments.** This study is based on the MS thesis research of Ford and was supported by NSF-MGG grant (0402685) to Schellenberg and Koch and GSA Student Grant to Ford. We thank the U.S National Park Service staff of the Cabrillo National Monument for field access and logistical support; Joan Kimbrough, Tony Carrasco, and Lisa Thurn of San Diego State University for analytical support; and the management and engineers of New Wave Research for working with us to integrate Bézier-curve-based microsampling paths and other modifications into their Micromill system. This manuscript benefited from the thoughtful critical reviews of L. Leighton, B. Hentschel, and two anonymous reviewers.

References

- Berner, R. A. (1975), Role of magnesium in crystal-growth of calcite and aragonite from sea-water, *Geochim. Cosmochim. Acta*, 39, 489–504, doi:10.1016/0016-7037(75)90102-7.
- Billups, K., and D. P. Schrag (2002), Paleotemperatures and ice volume of the past 27 Myr revisited with paired Mg/Ca and $^{18}\text{O}/^{16}\text{O}$ measurements on benthic foraminifera, *Paleoceanography*, 17(1), 1003, doi:10.1029/2000PA000567.
- Blanchette, C. A., B. Helmuth, and S. D. Gaines (2007), Spatial patterns of growth in the mus-

- sel, *Mytilus californianus*, across a major oceanographic and biogeographic boundary at Point Conception, California, USA, *J. Exp. Mar. Biol. Ecol.*, **340**, 126–148, doi:10.1016/j.jembe.2006.09.022.
- Carré, M., I. Bentaleb, O. Bruguier, E. Ordinola, N. T. Barrett, and M. Fontugne (2006), Calcification rate influence on trace element concentrations in aragonitic bivalve shells: Evidence and mechanisms, *Geochim. Cosmochim. Acta*, **70**, 4906–4920, doi:10.1016/j.gca.2006.07.019.
- Chauvaud, L., A. Lorrain, R. B. Dunbar, Y.-M. Paulet, G. Thouzeau, F. Jean, J.-M. Guarini, and D. Mucciarone (2005), Shell of the great scallop *Pecten maximus* as a high-frequency archive of paleoenvironmental changes, *Geochim. Geophys. Geosyst.*, **6**, Q08001, doi:10.1029/2004GC000890.
- Cohen, A. L., and S. R. Hart (2004), Deglacial sea surface temperatures of the western tropical Pacific: A new look at old coral, *Paleoceanography*, **19**, PA4031, doi:10.1029/2004PA001084.
- Cohen, A. L., and T. A. McConnaughey (2003), Geochemical perspectives on coral mineralization, in *Biominalization, Rev. Mineral. Geochim.*, vol. 54, edited by P. M. Dove, J. J. De Yoreo, and S. Weiner, pp. 151–187, Mineral. Soc. of Am., Washington, D. C.
- Craig, H., and L. I. Gordon (1965), Deuterium and oxygen 18 variations in the ocean and marine atmosphere, in *Proceedings of Stable Isotopes in Oceanographic Studies and Paleotemperatures*, edited by E. Tongiorgi, pp. 9–130, Cons. Naz. delle Ric., Rome.
- Crenshaw, M. A. (1972), Inorganic composition of molluscan extrapallial fluid, *Biol. Bull.*, **143**, 506–512, doi:10.2307/1540180.
- Crenshaw, M. A. (1980), Mechanisms of shell formation and dissolution, in *Skeletal Growth of Aquatic Organisms: Biological Records of Environmental Change*, edited by D. C. Rhoads and R. A. Lutz, pp. 115–128, Plenum, New York.
- Curriel-Ramírez, S., and J. Cáceres-Martínez (2004), Reproductive cycle of coexisting mussels, *Mytilus californianus* and *Mytilus galloprovincialis*, in Baja California, New Mexico, *J. Shellfish Res.*, **23**, 515–520.
- Dodd, R. J. (1965), Environmental control of strontium and magnesium in *Mytilus*, *Geochim. Cosmochim. Acta*, **29**, 385–398, doi:10.1016/0016-7037(65)90035-9.
- Drever, J. I. (1997), *The Geochemistry of Natural Waters*, 2nd ed., Prentice Hall, Englewood Cliffs, N. J.
- Dutton, A. L., K. C. Lohmann, and W. J. Zinsmeister (2002), Stable isotope and minor element proxies for Eocene climate of Seymour Island, Antarctica, *Paleoceanography*, **17**(2), 1016, doi:10.1029/2000PA000593.
- Epstein, S., R. Buchsbaum, H. A. Lowenstam, and H. C. Urey (1953), Revised carbonate-water isotopic temperature scale, *Geol. Soc. Am. Bull.*, **64**, 1315–1326, doi:10.1130/0016-7606(1953)64[1315:RCITS]2.0.CO;2.
- Freitas, P., L. J. Clarke, H. Kennedy, C. Richardson, and F. Abrantes (2005), Mg/Ca, Sr/Ca, and stable-isotope ($\delta^{18}\text{O}$ and $\delta^{13}\text{C}$) ratio profiles from the fan mussel *Pinna nobilis*: Seasonal records and temperature relationships, *Geochim. Geophys. Geosyst.*, **6**, Q04D14, doi:10.1029/2004GC000872.
- Freitas, P. S., L. J. Clarke, H. Kennedy, C. A. Richardson, and F. Abrantes (2006), Environmental and biological controls on elemental (Mg/Ca, Sr/Ca and Mn/Ca) ratios in shells of the king scallop *Pecten maximus*, *Geochim. Cosmochim. Acta*, **70**, 5119–5133, doi:10.1016/j.gca.2006.07.029.
- Freitas, P. S., L. J. Clarke, H. A. Kennedy, and C. A. Richardson (2008), Inter- and intraspecific variability masks reliable temperature control on shell Mg/Ca ratios in laboratory and field cultured *Mytilus edulis* and *Pecten maximus* (bivalvia), *Biogeosci. Discuss.*, **5**, 531–572.
- Gillikin, D. P., A. Lorrain, J. Navez, J. W. Taylor, L. André, E. Keppens, W. Baeyens, and F. Dehairs (2005), Strong biological controls on Sr/Ca ratios in aragonitic marine bivalve shells, *Geochim. Geophys. Geosyst.*, **6**, Q05009, doi:10.1029/2004GC000874.
- Goodkin, N. F., K. A. Huguen, and A. L. Cohen (2007), A multicoral calibration method to approximate a universal equation relating Sr/Ca and growth rate to sea surface temperature, *Paleoceanography*, **22**, PA1214, doi:10.1029/2006PA001312.
- Gordon, M., G. A. Knauer, and J. H. Martin (1980), *Mytilus californianus* as a bioindicator of trace metal pollution: Variability and statistical considerations, *Mar. Pollut. Bull.*, **11**, 195–198, doi:10.1016/0025-326X(80)90492-0.
- Gosling, E. M. (1992a), *Developments in Aquaculture and Fisheries Science*, vol. 25, *The Mussel Mytilus: Ecology, Physiology, Genetics and Culture*, 589 pp., Elsevier, Amsterdam.
- Gosling, E. M. (1992b), Systematics and geographic distribution of *Mytilus*, in *Developments in Aquaculture and Fisheries Science*, vol. 25, *The Mussel Mytilus: Ecology, Physiology, Genetics and Culture*, edited by E. Gosling, pp. 1–20, Elsevier, Amsterdam.
- Grossman, E. L., and T. L. Ku (1986), Oxygen and carbon isotope fractionation in biogenic aragonite: Temperature effects, *Chem. Geol.*, **59**, 59–74, doi:10.1016/0009-2541(86)90044-6.
- Horibe, Y., and T. Oba (1972), Temperature scales of aragonite-water and calcite-water systems, *Fossils*, **23–24**, 69–79.
- Kennett, D. J., B. L. Ingram, J. M. Erlanson, and P. Walker (1997), Evidence for temporal fluctuations in marine radiocarbon reservoir ages in the Santa Barbara Channel, southern California, *J. Archaeol. Sci.*, **24**, 1051–1059, doi:10.1006/jasc.1996.0184.
- Killingley, J. S. (1981), Seasonality of mollusk collecting determined from O-18 profiles of midden shells, *Am. Antiq.*, **46**, 152–158, doi:10.2307/279994.
- Killingley, J. S., and W. H. Berger (1979), Stable isotopes in a mollusk shell: Detection of upwelling events, *Science*, **205**, 186–188, doi:10.1126/science.205.4402.186.
- Killingley, J. S., and W. A. Newman (1982), ^{18}O fractionation in barnacle calcite: A barnacle paleotemperature equation, *J. Mar. Res.*, **40**, 893–902.
- Kim, S. T., and J. R. O'Neil (1997), Equilibrium and nonequilibrium oxygen isotope effects in synthetic carbonates, *Geochim. Cosmochim. Acta*, **61**, 3461–3475, doi:10.1016/S0016-7037(97)00169-5.
- Kirby, M. X., T. M. Soniat, and H. J. Spero (1998), Stable isotope sclerochronology of Pleistocene and recent oyster shells (*Crassostrea virginica*), *Palaaios*, **13**, 560–569, doi:10.2307/3515347.
- Klein, R. T., K. C. Lohmann, and C. W. Thayer (1996a), Bivalve skeletons record sea-surface temperature and $\delta^{18}\text{O}$ via Mg/Ca and $^{18}\text{O}/^{16}\text{O}$ ratios, *Geology*, **24**, 415–418, doi:10.1130/0091-7613(1996)024<0415:BSRSSST>2.3.CO;2.
- Klein, R. T., K. C. Lohmann, and C. W. Thayer (1996b), Sr/Ca and $^{13}\text{C}/^{12}\text{C}$ ratios in skeletal calcite of *Mytilus trossulus*: Covariation with metabolic rate, salinity, and carbon isotopic composition of seawater, *Geochim. Cosmochim. Acta*, **60**, 4207–4221, doi:10.1016/S0016-7037(96)00232-3.
- Klein, R. T., K. C. Lohmann, and G. L. Kennedy (1997), Elemental and isotopic proxies of paleotemperature and paleosalinity: Climate reconstruction of the marginal northeast Pacific ca. 80 ka, *Geology*, **25**, 363–366, doi:10.1130/0091-7613(1997)025<0363:EAIPOP>2.3.CO;2.
- Lansman, J. B., P. Hess, and R. W. Tsien (1986), Blockade of current through single calcium channels by Cd^{2+} , Mg^{2+} , and Ca^{2+} : Voltage and concentration dependence of calcium entry into the pore, *J. Gen. Physiol.*, **88**, 321–347, doi:10.1085/jgp.88.3.321.
- Lea, D. W. (2003), Elemental and isotopic proxies of marine temperatures, in *Treatise on Geochemistry*, vol. 6, *The Oceans and Marine Geochemistry*, edited by H. Elderfield, pp. 365–390, Elsevier, Oxford, U. K.
- Lea, D. W., D. K. Pak, and H. J. Spero (2000), Climate impact of Late Quaternary equatorial Pacific sea surface temperature variations, *Science*, **289**, 1719–1724, doi:10.1126/science.289.5485.1719.
- Lear, C. H., H. Elderfield, and P. A. Wilson (2000), Cenozoic deep-sea temperatures and global ice volumes from Mg/Ca in benthic foraminiferal calcite, *Science*, **287**, 269–272, doi:10.1126/science.287.5451.269.
- Lorrain, A., D. P. Gillikin, Y. Paulet, L. Chauvaud, A. L. Mercier, J. Navez, and L. André (2005), Strong kinetic effects on Sr/Ca ratios in the calcitic bivalve *Pecten maximus*, *Geology*, **33**, 965–968, doi:10.1130/G22048.1.
- McConnaughey, T. (1989a), ^{13}C and ^{18}O isotopic disequilibrium in biological carbonates: I. Patterns, *Geochim. Cosmochim. Acta*, **53**, 151–162, doi:10.1016/0016-7037(89)90282-2.
- McConnaughey, T. (1989b), ^{13}C and ^{18}O isotopic disequilibrium in biological carbonates: II. In vitro simulation of kinetic isotope effects, *Geochim. Cosmochim. Acta*, **53**, 163–171, doi:10.1016/0016-7037(89)90283-4.
- Owen, R., H. Kennedy, and C. Richardson (2002a), Isotopic partitioning between scallop shell calcite and seawater: Effect of shell growth rate, *Geochim. Cosmochim. Acta*, **66**, 1727–1737, doi:10.1016/S0016-7037(01)00882-1.
- Owen, R., H. Kennedy, and C. Richardson (2002b), Experimental investigation into partitioning of stable isotopes between scallop (*Pecten maximus*) shell calcite and sea water, *Palaeoogeogr. Palaeoecolimatol. Palaeoecol.*, **185**, 163–174, doi:10.1016/S0031-0182(02)00297-3.
- Page, H. M., and D. M. Hubbard (1987), Temporal and spatial patterns of growth in mussels *Mytilus edulis* on an offshore platform: Relationships to water temperature and food availability, *J. Exp. Mar. Biol. Ecol.*, **111**, 159–179, doi:10.1016/0022-0981(87)90053-0.
- Petersen, J. H. (1984), Larval settlement behavior in competing species: *Mytilus californianus* Conrad and *M. edulis* L., *J. Exp. Mar. Biol. Ecol.*, **82**, 147–159, doi:10.1016/0022-0981(84)90100-X.
- Purton, L. M. A., G. A. Shields, M. D. Brasier, and G. W. Grime (1999), Metabolism controls Sr/Ca ratios in fossil aragonitic mollusks, *Geology*, **27**, 1083–1086, doi:10.1130/0091-7613(1999)027<1083:MCSCRI>2.3.CO;2.

- Richardson, C. A. (1989), An analysis of the microgrowth bands in the shell of the common mussel *Mytilus edulis*, *J. Mar. Biol. Assoc. U. K.*, **69**, 477–491, doi:10.1017/S0025315400029544.
- Robertson, J. D. (1964), Osmotic and ionic regulation, in *Physiology of Mollusca*, vol. 1, edited by K. Wilbur and C. M. Yonge, pp. 283–311, Academic, London.
- Rosenberg, G. D., and W. W. Hughes (1991), A metabolic model for the determination of shell composition in the bivalve mollusc, *Mytilus edulis*, *Lethaia*, **24**, 83–96, doi:10.1111/j.1502-3931.1991.tb01182.x.
- Schifano, G., and P. Censi (1983), Oxygen isotope composition and rate of growth of *Patella coerulea*, *Monodonta turbinata* and *M. articulata* shells from the western coast of Sicily, *Palaeogeogr. Palaeoclimatol. Palaeoecol.*, **42**, 305–311, doi:10.1016/0031-0182(83)90028-7.
- Schifano, G., and P. Censi (1986), Oxygen and carbon isotope composition, magnesium and strontium contents of calcite from a subtidal *Patella coerulea* shell, *Chem. Geol.*, **58**, 325–331.
- Seed, R., and T. H. Suchanek (1992), Population of community ecology of *Mytilus*, in *Developments in Aquaculture and Fisheries Science*, vol. 25, *The Mussel Mytilus: Ecology, Physiology, Genetics and Culture*, edited by E. Gosling, pp. 87–169, Elsevier, Amsterdam.
- Sosdian, S., D. K. Gentry, C. H. Lear, E. L. Grossman, D. Hicks, and Y. Rosenthal (2006), Strontium to calcium ratios in the marine gastropod *Conus ermineus*: Growth rate effects and temperature calibration, *Geochem. Geophys. Geosyst.*, **7**, Q11023, doi:10.1029/2005GC001233.
- Spangenberg, J. V., and G. N. Cherr (1996), Developmental effects of barium exposure in a marine bivalve (*Mytilus californianus*), *Environ. Toxicol. Chem.*, **15**, 1769–1774.
- Spero, H. J., J. Bijma, D. W. Lea, and B. E. Bemis (1997), Effect of seawater carbonate concentration on foraminiferal carbon and oxygen isotopes, *Nature*, **390**, 497–500, doi:10.1038/37333.
- Suchanek, T. H. (1981), The role of disturbance in the evolution of life history strategies in the intertidal mussels *Mytilus edulis* and *Mytilus californianus*, *Oecologia*, **50**, 143–152, doi:10.1007/BF00348028.
- Suchanek, T. H., J. B. Geller, B. R. Kresier, and J. B. Mitton (1997), Zoogeographic distributions of the sibling species *Mytilus galloprovincialis* and *M. trossulus* (Bivalvia: Mytilidae) and their hybrids in the North Pacific, *Biol. Bull.*, **193**, 187–194, doi:10.2307/1542764.
- Surge, D., and K. J. Walker (2006), Geochemical variation in microstructural shell layers of the southern quahog (*Mercenaria campechiensis*): Implications for reconstructing seasonality, *Palaeogeogr. Palaeoclimatol. Palaeoecol.*, **237**, 182–190, doi:10.1016/j.palaeo.2005.11.016.
- Surge, D., K. C. Lohmann, and D. L. Dettman (2001), Controls on isotopic chemistry of the American oyster, *Crassostrea virginica*: Implications for growth patterns, *Palaeogeogr. Palaeoclimatol. Palaeoecol.*, **172**, 283–296, doi:10.1016/S0031-0182(01)00303-0.
- Takesue, R. K., and A. Van Geen (2004), Mg/Ca, Sr/Ca, and stable isotopes in modern and Holocene *Protothaca staminea* shells from a northern California coastal upwelling region, *Geochim. Cosmochim. Acta*, **68**, 3845–3861, doi:10.1016/j.gca.2004.03.021.
- Taylor, J. D., W. J. Kennedy, and A. Hall (1969), *The Shell Structure and Mineralogy of the Bivalvia: Introduction—Nuculacea-Trigonacea*, *Bull. Br. Mus. (Nat. Hist.)*, **Zool.**, **3**, 125 pp.
- Thébault, J., L. Chauvaud, J. Clavier, J. Guarini, R. B. Dunbar, R. Fichez, D. A. Mucciarone, and E. Morize (2007), Reconstruction of seasonal temperature variability in the tropical Pacific Ocean from the shell of the scallop, *Comptopallium radula*, *Geochim. Cosmochim. Acta*, **71**, 918–928, doi:10.1016/j.gca.2006.10.017.
- Urey, H. C. (1947), The thermodynamic properties of isotopic substances, *J. Chem.*, **562**–581, doi:10.1039/jr9470000562.
- Vander Putten, E., F. Dehairs, E. Keppens, and W. Baeyens (2000), High resolution distribution of trace elements in the calcite shell layer of modern *Mytilus edulis*: Environmental and biological controls, *Geochim. Cosmochim. Acta*, **64**, 997–1011, doi:10.1016/S0016-7037(99)00380-4.
- Walker, P. L., D. J. Kennett, T. L. Jones, and R. DeLong (1999), Archaeological investigations at the Point Bennett pinniped rookery on San Miguel Island, in *Proceedings of the Fifth California Islands Symposium*, edited by D. R. Brown, K. L. Mitchell, and H. W. Chaney, pp. 628–632, Santa Barbara Mus. of Nat. Hist., Santa Barbara, Calif.
- Wanamaker, A. D., Jr., K. J. Kreutz, H. W. Borns Jr., D. S. Introne, S. Feindel, and B. J. Barber (2006), An aquaculture-based method for calibrated bivalve isotope paleothermometry, *Geochem. Geophys. Geosyst.*, **7**, Q09011, doi:10.1029/2005GC001189.
- Wanamaker, A. D., Jr., K. J. Kreutz, H. W. Borns Jr., D. S. Introne, S. Feindel, S. Funder, P. D. Rawson, and B. J. Barber (2007), Experimental determination of salinity, temperature, growth, and metabolic effects on shell isotope chemistry of *Mytilus edulis* collected from Maine and Greenland, *Paleoceanography*, **22**, PA2217, doi:10.1029/2006PA001352.
- Wefer, G., and W. H. Berger (1991), Isotope paleontology: Growth and composition of extant calcareous species, *Mar. Geol.*, **100**, 207–248, doi:10.1016/0025-3227(91)90234-U.
- Wheeler, A. P. (1992), Mechanisms of molluscan shell formation, in *Calcification in Biological Systems*, edited by E. Bonucci, pp. 179–215, CRC Press, Boca Raton, Fla.
- Zeebe, R. E. (1999), An explanation of the effect of seawater carbonate concentration on foraminiferal oxygen isotopes, *Geochim. Cosmochim. Acta*, **63**, 2001–2007, doi:10.1016/S0016-7037(99)00091-5.

B. J. Becker, Department of Environmental Sciences, University of Washington, 1900 Commerce St., Box 358436, Tacoma, WA 98402, USA.

D. L. Deutschman, Department of Biological Sciences, San Diego State University, 5500 Campanile Dr., San Diego, CA 92182, USA.

K. A. Dyck and P. L. Koch, Department of Earth Sciences, University of California, 1156 High St., Santa Cruz, CA 95064, USA.

H. L. Ford, Department of Ocean Sciences, University of California, 1156 High St., Santa Cruz, CA 95064, USA.

S. A. Schellenberg, Department of Geological Sciences, San Diego State University, 5500 Campanile Dr., San Diego, CA 92182, USA. (schellenberg@geology.sdsu.edu)